

Transient non-linear response of ‘pull-in MEMS devices’ including squeeze film effects

M.H.H. Oude Nijhuis, T.G.H. Basten, Y.H. Wijnant, H.Tijdeman and H.A.C. Tilmans*

University of Twente, Department of Mechanical Engineering, P.O. Box 217,
7500 AE Enschede, The Netherlands

*CP Clare N.V., B-3500 Hasselt, Belgium

E-mail: m.h.h.oudenijhuis@wb.utwente.nl

SUMMARY

The dynamic behaviour of “pull-in MEMS devices” including a squeeze film is described by non-linear differential equations that are solved numerically. The pull-in time of a basic parallel plate structure as a function of the ambient pressure, external driving force and plate length/width ratio has been simulated for single- and double-gap configurations. It has been found that the pull-in time can be greatly reduced by lowering the ambient pressure and/or by increasing the driving force. The model has been applied to predict the operate time of an electromagnetic microrelay. Measurements and simulations show good agreement.

Keywords: pull-in dynamics, microrelay, squeeze film effect, numerical simulation.

INTRODUCTION

The dynamic behaviour of ‘pull-in MEMS devices’, such as deformable micromirrors [1] and microrelays [2,3,4], strongly depends on squeeze film effects due to gas trapped in a narrow gap. These devices are typically parallel plate devices which are operated in a contact/non-contact mode, whereby a movable plate collapses against another stationary plate as a result of an electrostatic or electromagnetic force. The gas trapped in the narrow gap separating the two plates has a very strong influence on the pull-in time, i.e. the time it takes to bring the two plates into intimate contact. Closing the gap results in a pressure disturbance in the gas film, leading to the so-called squeeze film force, which opposes the motion of the plate.

Previous studies on the pull-in behaviour in the presence of a squeeze film have been reported [5,6]. Hung et al. [5] discuss a similar model as presented here, but focus on optimizing numerical simulation times, and not so much on the results. Gupta et al. [6] present a model based on a single-degree-of-freedom system, thereby assuming a squeeze film force which is proportional to the velocity of the plate. In the present paper this assumption is not made. Instead, the squeeze film force is derived from the compressible Reynolds equation. Further in [6], some parameters are determined based on experimental results. In the present model, all parameters are obtained from the design of the structure, rendering the model more suitable as a design tool. The model is validated by comparing the simulated and measured pull-in dynamics of an electromagnetic microrelay [3,4].

DYNAMIC MODELLING

The model will be described for the system depicted in Fig. 1, but is applicable to more complicated systems. Under the assumption of a rigid plate moving along the z -axis, the equation of motion of the system is given by

$$m\ddot{h} - k(h_0 - h) - F_d = -F_{ext}, \quad (1)$$

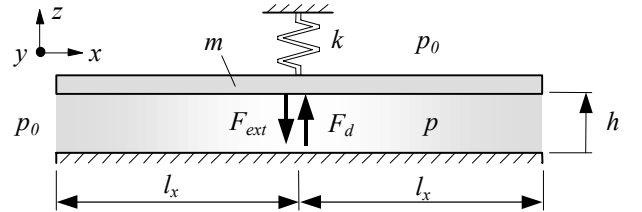


Fig. 1: Mass-spring system including squeeze film effects.

where $h=h(t)$ is the gap spacing defining the thickness of the squeeze film, h_0 is the initial gap spacing, m is the mass of the plate, k is the linear spring stiffness, F_d is the squeeze film force, and F_{ext} is an externally applied closing force. In the case of pull-in devices, F_{ext} is a non-linear force of electrostatic or electromagnetic origin. The expressions for F_{ext} for a single gap device are given in Table 1 for both cases.

Table 1: Electrostatic and electromagnetic force [7].

electrostatic ($\epsilon_r=1$ in gap)	electromagnetic ($\mu_r \rightarrow \infty$ in yoke)
$F_{ext} = \frac{\epsilon_0 A V^2}{2 h^2}$	$F_{ext} = \frac{\mu_0 A (NI)^2}{2 h^2}$

In the case of an electrostatic closing force, the parameters involved are the permittivity of vacuum ϵ_0 , the electrode area A , and the applied voltage V . For its electromagnetic counterpart, the parameters are the permeability of vacuum μ_0 , the pole area A , the number of coil windings N , and the applied current I . In the remaining part of the paper, the analysis will be restricted to an electromagnetic device, but because of the electrostatic-electromagnetic analogy, the model can easily be interpreted for the electrostatic case.

The squeeze film force resulting from the pressure disturbance in the narrow gap is given by

$$F_d = \int_{-l_y}^{l_y} \int_{-l_x}^{l_x} (p - p_0) dx dy, \quad (2)$$

where $p=p(x,y,t)$ is the pressure distribution in the gap, and l_x and l_y are the half plate lengths in the x - and y -direction respectively. The ambient pressure p_0 is the initial pressure in the gas film. The pressure at the edges of the plate is assumed to be p_0 during the whole motion. The pressure in the gas film is derived from the compressible isothermal Reynolds equation [8]

$$\frac{\partial}{\partial x} \left(\frac{ph^3}{12\eta} \frac{\partial p}{\partial x} \right) + \frac{\partial}{\partial y} \left(\frac{ph^3}{12\eta} \frac{\partial p}{\partial y} \right) = \frac{\partial(ph)}{\partial t}, \quad (3)$$

where η is the viscosity of the gas. Equation (3) is derived from the Navier-Stokes equation and the continuity equation, assuming that (i) the gap is narrow ($h \ll l_x, l_y$), (ii) the inertial effects are negligible compared to the viscous effects of the flow, and, (iii) a perfect gas is considered that behaves isothermally. As a result of these assumptions, the pressure is independent of the z -coordinate.

When gap spacings are on the order of the molecular mean free path of the gas, the so-called ‘slip’ of the gas along the walls must be accounted for [9]. This effect can be modelled by an effective viscosity, which is given by

$$\eta = \frac{\eta_0}{1 + f(K_n)}, \quad (4)$$

where $K_n = (p_0 \lambda_0)/(p h)$ is the Knudsen number, η_0 is the viscosity at pressure p_0 , and λ_0 is the mean free path at pressure p_0 . Because the mean free path is inversely proportional to the pressure, molecular slip becomes especially important at low pressures. Several definitions of the function $f(K_n)$ can be found in the literature [10]. In this work $f(K_n) = 6K_n$ according to Burgdorfer [9] is used.

Because equations (1) and (3) are strongly coupled and non-linear, analytical solutions for h and p cannot be found. Numerical techniques are therefore applied. The Reynolds equation is discretized with a second order finite difference scheme, while the equation of motion is solved using the Newmark time-integration scheme [11].

SIMULATION RESULTS

In this section, simulation results for a fictitious device represented by the structure in Fig. 1 are presented. The input parameters being representative for pull-in MEMS device are given in Table 2. Fig. 2 shows the time history of the gap height and the maximum pressure in the gap for two different values of the magnetomotive force NI . As the gap decreases, the pressure in the gap increases. The simulated pressure approaches infinity as the plates come into intimate contact. The step response of the gapheight is very much similar to the response given in [5]. A typical pressure distribution plot is shown in Fig. 3. Because of the parallel plate assumption, the maximum pressure occurs at the plate center ($x=y=0$).

Table 2: Parameters as used for Figs. 2-7.

$NI = 1.0 \text{ A}\cdot\text{T(urns)}$	$l_x = 1.0 \cdot 10^{-3} \text{ m}$
$\mu_0 A/2 = 1.3 \cdot 10^{-3} \text{ H}\cdot\text{m}$	$l_y = 1.0 \cdot 10^{-3} \text{ m}$
$k = 40 \text{ N}\cdot\text{m}^{-1}$	$p_0 = 1.0 \cdot 10^5 \text{ Pa}$
$m = 1.0 \cdot 10^{-6} \text{ kg}$	$\eta_0 = 1.8 \cdot 10^{-5} \text{ Pa}\cdot\text{s}$
$h_0 = 2.5 \cdot 10^{-3} \text{ m}$	$\lambda_0 = 6.4 \cdot 10^{-8} \text{ m}$

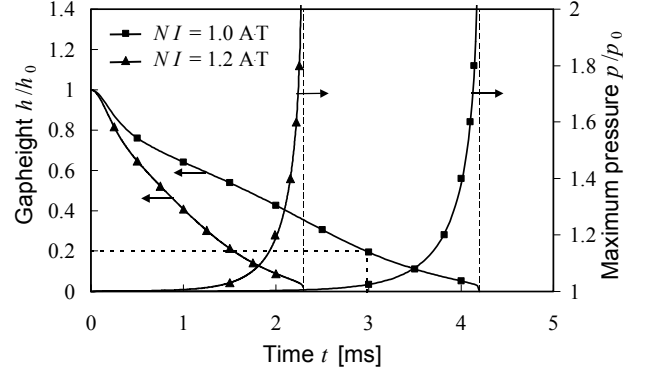


Fig. 2: Simulated step response of the gap height and the pressure for two magnetomotive forces applied at $t = 0$ s.

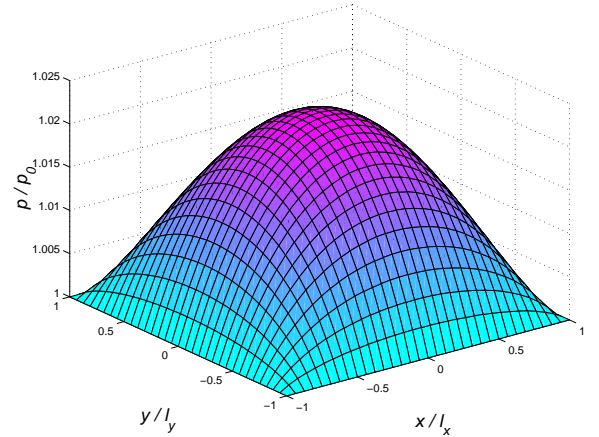


Fig. 3: Simulated gap pressure distribution on $t = 3.0$ ms for $NI = 1 \text{ A}\cdot\text{T}$.

In many pull-in MEMS devices, e.g. the microrelay described in [4], the gap will not reduce to zero. Instead, the motion of the plate is limited by ‘bumps’ with a height h_c (see section electromagnetic microrelay). The pull-in time is thus conveniently defined as the time it takes to move the plate from its initial position $h=h_0$ to contact closure $h=h_c$. The results presented in the remaining part of this section are derived for $h_c=0.5$ micron, i.e. $h_c/h_0=0.2$.

Fig. 4 shows the pull-in time as a function of the magnetomotive force. A minimum driving force is needed for contact closure. This value can be approximated by the quasi-static pull-in force $NI_{PI} = \sqrt{(8kh_0^3)/(27\mu_0 A)}$ [7].

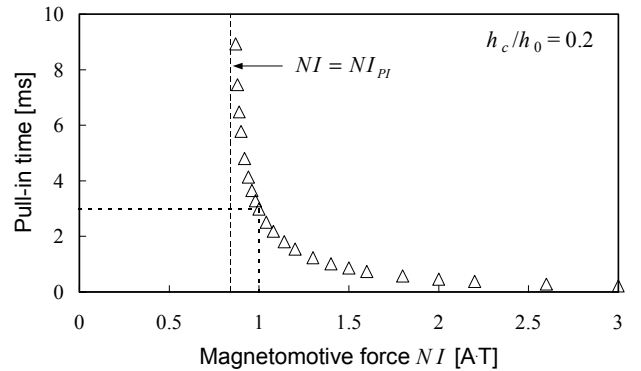


Fig. 4: Simulated pull-in time vs. the magnetomotive force NI .

The pull-in time is also simulated as a function of the ambient pressure. Fig. 5 shows that at low pressures, the pull-in time asymptotically approaches the pull-in time in vacuum. For higher pressures, the squeeze film effect becomes dominant. At atmospheric conditions, the pull-in time is about six times larger than the pull-in time in vacuum. Fig. 5 also illustrates that around 1000 Pa, the assumption slip versus no-slip has a significant effect on the simulated pull-in time. For the given set of parameters, which is typical for pull-in MEMS devices, slip of the gas along the walls can clearly not be neglected for a wide intermediate pressure range.

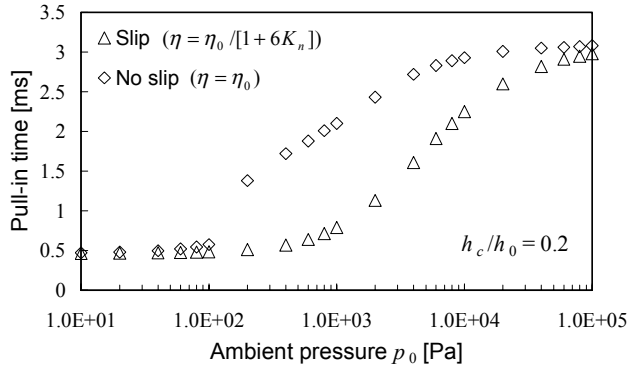


Fig. 5: Simulated pull-in time vs. the ambient pressure simulated with slip and no-slip boundary conditions.

The pull-in time is further simulated for different values of the plate aspect ratio l_x/l_y , whereby the plate area remains the same. Fig. 6 shows that the squeeze film effect is maximal for a square plate. It is pointed out, that the aspect ratio may freely be varied as long as the condition $h \ll l_x, l_y$ remains fulfilled. For large aspect ratios, the results are well approximated by the one dimensional Reynolds equation [8].

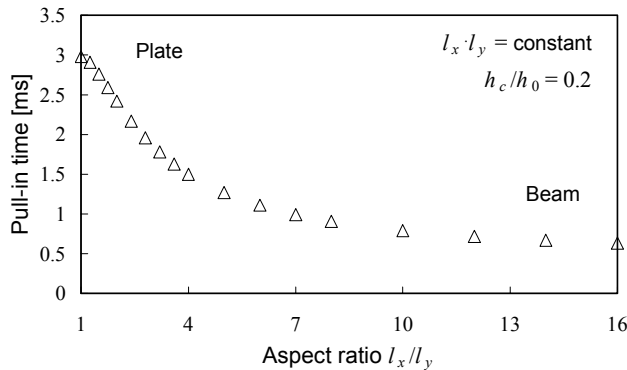


Fig. 6: Simulated pull-in time vs. the aspect ratio l_x/l_y .

DOUBLE-GAP MODEL

In many pull-in MEMS devices, for example the microrelay discussed in the next section, the motion of the plate is opposed by a second squeeze film. In order to solve such a 'double-gap' problem, a second Reynolds equation is added to the foregoing model. Fig. 7 shows the pull-in time for a downward motion of the plate versus the ratio $h_{2,0}/h_{1,0}$, where $h_{1,0}$ is the initial lower gapheight and $h_{2,0}$ is the initial upper gapheight. It is noted, that $h_{2,0}$ is varied while keeping $h_{1,0}$ constant. The pull-in time shows a strong increase with decreasing $h_{2,0}/h_{1,0}$. When $h_{2,0}/h_{1,0}$

exceeds unity, the pull-in time approximates the pull-in time of the single-gap model. When the initial upper gapheight is more than two times larger than the initial lower gapheight, the influence of the upper film may be neglected.

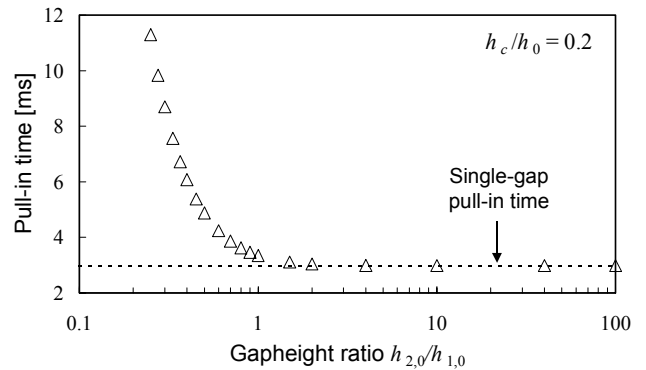


Fig. 7: Simulated pull-in time vs. ratio of initial upper and lower gap height. The other model parameters are given in Table 2.

ELECTROMAGNETIC MICRORELAY

The electromagnetic microrelay depicted in Fig. 1 comprises an example of a double gap structure [3,4]. In this section, the pull-in time or more appropriate, the first operate time, of the microrelay is simulated using the foregoing model. A current in the coil induces an electromagnetic force exerted on the keeper via the poles. This results in a closure of the electrical contacts. Note that the first operate time is the time it takes to induce first contact closure. Hence, bounce is excluded. The system has two gaps: one between the upper substrate and the keeper and one between the keeper and the bottom FeSi substrate.

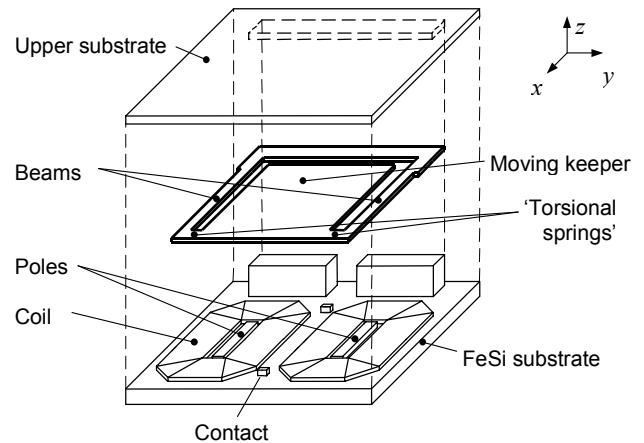


Fig. 8: Schematic drawing of a microrelay [3,4].

The in-plane dimensions are on the order of millimetres whereas the gap spacings are in the micron range resulting in strong squeeze film effects. Details on dimensions can be found in [4]. The keeper is modelled as a rigid plate supported by two elastic beams which are connected to the keeper via torsional springs as shown in Fig. 9. The overall spring constant is composed of the stiffness of the elastic beams and the torsional springs. Compared to the system depicted in Fig. 1, additional degrees of freedom are introduced to simulate the motion of the keeper.

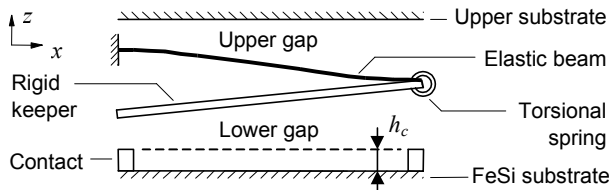


Fig. 9: 2D-view of the microrelay model.

Graphs of the measured and simulated first operate times as functions of the ambient pressure for three different driving voltages are shown in Fig. 10. The simulated results show reasonable agreement with the measurements. At low pressures, the first operate time is fully determined by the inertia of the keeper and the actuation force. At higher pressures, the squeeze film effect becomes dominant. The graph indicates that the first operate time of the microrelay can be improved by almost one order of magnitude when the pressure is decreased by two orders of magnitude (starting from the ambient pressure).

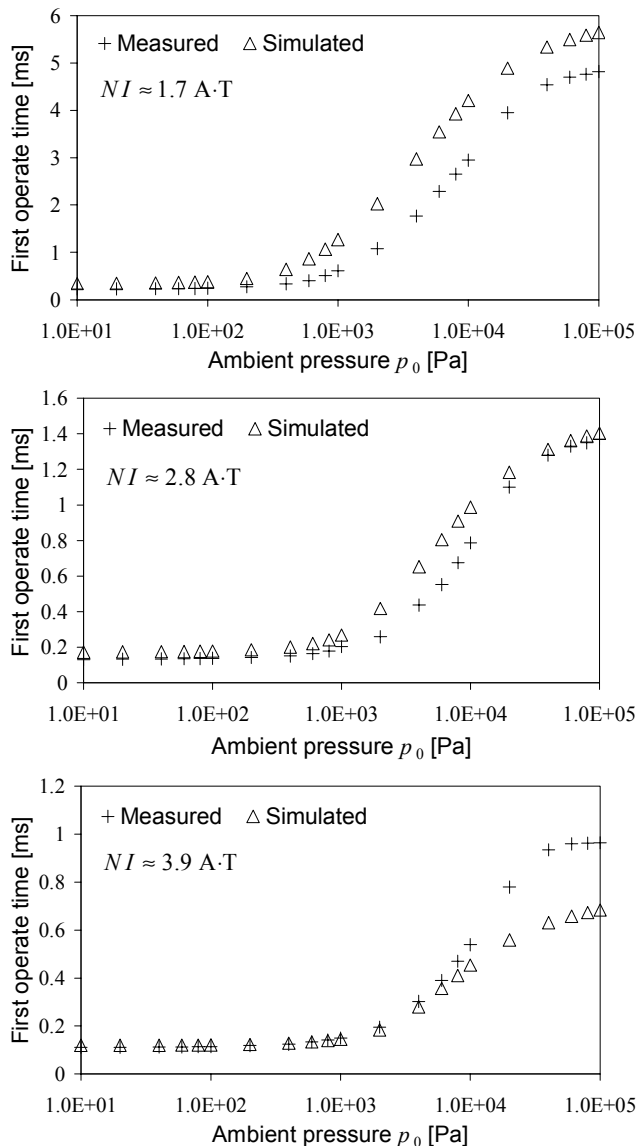


Fig. 10: Measured and simulated results of the first operate time versus the ambient pressure for coil voltages of 3 V ($NI \approx 1.7$ A·T), 5 V ($NI \approx 2.8$ A·T) and 7 V ($NI \approx 3.9$ A·T).

CONCLUSIONS

A model describing the non-linear dynamic behaviour of pull-in MEMS devices including a squeeze film has been presented. Pull-in times can be significantly reduced by lowering the ambient pressure and/or by increasing the driving signal. Simulation results of the first operate time of an electromagnetic microrelay show good agreement with measurements. The model can be used as a design tool to predict the dynamical behaviour of a variety of MEMS structures which involve a squeeze film.

ACKNOWLEDGMENTS

This work has in part been sponsored by the European Commission in the frame of the ESPRIT programme (MIRS project 20679). The authors further acknowledge the valuable input of the other partners in MIRS: CSEM (Switzerland), ARITECH (The Netherlands), IMEC (Belgium), and SPEA (Italy). Special thanks to T.J.S. Lammerink and R.G.P. Sanders from the MESA Research Institute for supervising the measurements.

REFERENCES

- [1] L.J. Hornbeck, 128 x 128 deformable mirror device, *IEEE Transactions on Electron Devices*, ED-30, 1983, p. 539.
- [2] M.-A. Grétilat, Y.-J. Yang, E.S. Hung, V. Rabinovich, G.K. Ananthasuresh, N.F. de Rooij and S.D. Senturia, Nonlinear electromechanical behavior of an electrostatic microrelay, *Proc. Transducers '97*, Chicago, Illinois, USA, June 16-19, 1997, pp. 1141-1144.
- [3] E. Fullin, J. Gobet, H.A.C. Tilmans, and J. Berqvist, A new basic technology for magnetic micro-actuators, *Proc. MEMS '98*, Heidelberg, Germany, Jan. 25-29, 1998, pp. 143-147.
- [4] H.A.C. Tilmans, E. Fullin, H. Ziad, M.D.J. Van de Peer, J. Kesters, E. Van Geffen, J. Berqvist, M. Pantus, E. Beyne, K. Baert, and F. Naso, A fully-packaged electromagnetic microrelay, *Proc. MEMS '99*, Orlando, Florida, USA, Jan. 17-21, 1999, pp. 25-30.
- [5] E.S. Hung, Y.-J. Yang and S.D. Senturia, Low-order models for fast dynamical simulation of MEMS microstructures, *Proc. Transducers '97*, Chicago, Illinois, USA, June 16-19, 1997, pp. 1101-1104.
- [6] R.K. Gupta and S.D. Senturia, Pull-in time dynamics as a measure of absolute pressure, *Proc. MEMS '97*, Nagoya, Japan, Jan. 26-30, 1997, pp. 290-294.
- [7] H.H. Woodson and J.R. Melcher, *Electromechanical dynamics*, Wiley, New York, part I, II and III, 1968.
- [8] V.N. Constantinescu, *Gas lubrication*, ASME, New York, 1996.
- [9] A. Burgdorfer, The influence of the molecular mean free path on the performance of hydrodynamic gas lubricated bearings, *J. of Basic Engineering*, Vol. 81, 1959, pp. 94-99.
- [10] T. Veijola, H. Kuisma, J. Lahdenperä and T. Ryhänen, Equivalent-circuit model of the squeezed gas film in a silicon accelerometer, *Sensors and Actuators A*, 48, 1995, pp. 239-248.
- [11] K.J. Bathe, *Finite element procedures in engineering analysis*, Prentice Hall Inc..